

Reversal of magnetization of a single-domain magnetic particle by the ac field of time-dependent frequency

Liufei Cai, D. A. Garanin, and E. M. Chudnovsky
Physics Department, Lehman College, City University of New York
250 Bedford Park Boulevard West, Bronx, New York 10468-1589, USA

(Dated: October 31, 2018)

We report numerical and analytical studies of the reversal of the magnetic moment of a single-domain magnetic particle by a circularly polarized ac field of time-dependent frequency. For the time-linear frequency sweep, the phase diagrams are computed that illustrate the dependence of the reversal on the frequency sweep rate v , the amplitude of the ac field h , the magnetic anisotropy field d , and the damping parameter α . It is shown that the most efficient magnetization reversal requires a non-linear time dependence of the frequency, $\omega(t)$, for which an exact analytical formula is derived with account of damping. The necessary condition of the reversal is $h > \alpha d$. Implementation of a small-scale magnetization reversal is proposed in which a nanomagnet is electromagnetically coupled to two weak superconducting links controlled by the voltage. Dynamics of such a system is analyzed with account of the back effect of the magnet on the superconducting links.

PACS numbers: 75.60.Jk, 84.40.-x, 75.50.Tt, 85.25.Cp

I. INTRODUCTION

In recent years a significant effort has been made to achieve magnetization reversal in nanostructures, assisted by the low amplitude ac field in the radio frequency range. The idea is rather simple. The dc magnetic field required to reverse the magnetization of a single-domain magnetic particle, the so-called anisotropy field, is typically in the range 0.01-0.1T. The field of this strength at the location of the particle is not easy to develop fast. The ac magnetic field that one can typically develop in the radio-frequency range would be two orders of magnitude weaker. Applied in a resonant fashion, it could increase the amplitude of the precession of the magnetic moment, sometimes leading to its full reversal, in the same way as weak pushes of a pendulum at the frequency of its mechanical oscillation can flip the pendulum over the top. However, the study of both problem shows a lack of robust reversal. In many cases the attempted reversal results in a chaotic behavior that may be interesting on its own.

Magnetization reversal by ultrashort magnetic field pulses produced by a high-energy electron beam has been studied by Back et al.¹ in perpendicularly magnetized CoPt films. Schumacher et al² studied phase coherent precessional magnetization reversal in spin valves by a pulse of the transverse field of a few hundred picosecond duration produced by the electric current.

Later, significant number of experiments focused on microwave-assisted reversal in smaller structures and individual single-domain magnets with a strong static field applied to reduce the barrier. Thirion et al³ attempted magnetization reversal in static fields below the anisotropy field, assisted by a linearly polarized microwave field, in 20-nm-diameter Co particles placed on the bridge of a micro-SQUID. They were able to reproduce the Stoner-Wohlfarth astroid⁴ and study the dependence of the reversal on the frequency and duration

of the ac pulse. Enhancement of the magnetization reversal by microwave magnetic fields in nanometer Co strips has been demonstrated by Grollier et al.⁶ Nembach et al⁷ and Nozaki et al⁸ used magnetic force microscopy to measure microwave assisted magnetization reversal in individual submicron Co and permalloy particles. Microwave-assisted magnetization switching in permalloy tunnel junctions has been demonstrated by Moriyama et al⁹. Podbielski et al studied magnetization reversal in microscopic permalloy rings at GHz frequency. They observed non-linear spin dynamics and obtained experimental phase diagram of the reversal as function of microwave frequency and power.¹⁰ Using time-resolved magneto-optic Kerr microscopy, Woltersdorf and Back¹¹ detected enhancement of magnetization switching in single-domain permalloy elements subjected to the resonant microwave field. Microwave-assisted magnetization reversal in single-domain permalloy nanoelements has been studied by Nembach et al.¹³ Wang et al¹⁴ have investigated experimentally the competition between damping and pumping for microwave-assisted magnetization reversal in FeCo thin films.

Theoretical research in this area mostly focused on the magnetization reversal assisted by the ac field of constant frequency.¹⁵ Non-linear magnetization dynamics induced by such a field that results in a chaotic behavior has been studied by Bertotti et al.^{16,17} Denisov et al¹⁸ addressed magnetization of nanoparticles in a rotating magnetic field. Synchronization and chaos induced in the damped dynamics of a single-domain particle by the ac field of constant frequency has been investigated by Sun and Wang.⁵ Nonlinear-dynamical-system approach to the microwave-assisted magnetization dynamics was reviewed by Bertotti et al.¹⁵ Micromagnetic modelling of microwave-assisted magnetic recording was performed by Wang et al.¹² Constant frequency microwave switching magnetic grains coupled by exchange interaction has been investigated by Igarashi et al.¹⁹ Okamoto et al ad-

dressed stability of the magnetization switching by linearly and circularly polarized waves. Magnetization reversal in a resonant cavity has been studied by Yukalov and Yukalova.²²

Fewer number of theoretical papers have considered dynamics of the magnetization of a nanoparticle generated by the ac magnetic field of variable frequency. Mayergoltz et al²³ developed the inverse problem approach to the precessional switching of the magnetization by a linearly polarized pulse of the magnetic field. Rivkin and Ketterson²⁴ obtained the optimal time dependence of the microwave frequency in the absence of damping, as well as the condition of the reversal in the presence of damping. Magnetization reversal by a linearly polarized ac field of frequency that depends linearly on time has been studied by two of the authors.²⁵ Barros et al²¹ developed an optimization method in which the energy consumption needed for reversal is minimized with respect to the time dependence of the amplitude and frequency of microwaves.

A few general points need to be made before addressing the problem of the reversal of the magnetization by the microwaves. Firstly, a robust magnetization reversal can be effectively achieved only with a circularly polarized ac field. Indeed, photons of circular polarization have a definite orientation of their spin projection, while photons with linear polarization are in a superposition of spin states. Consequently, photons with the right circular polarization, when absorbed by the magnet, drive the magnetization in one direction towards the reversal, while linearly polarized photons can be both absorbed and emitted and, therefore, do not necessarily reverse the magnetization. Secondly, the photons are effectively absorbed only when they are in resonance with the spin levels. The latter are not equidistant on the magnetic quantum number, that is, on the projection of the magnetic moment on the direction of the effective field. Thus, as the magnetic moment reverses, the photon frequency that can be resonantly absorbed by the magnet changes with time, so that the frequency of the microwave field has to be adjusted. Damping of the precession adds another dimension to this problem as the power of the ac field that is pumped into the magnet should exceed the rate of energy dissipation. Analysis shows that circularly polarized small-amplitude ac field of a time-dependent frequency that follows the condition of the resonance is sufficient for achieving magnetization reversal. The case of a zero static field is of the highest practical importance.

The typical wavelength of microwaves that are in resonance with the precession of the magnetic moment is in the centimeter range. Thus, one of the challenges for potential applications of the microwave-assisted magnetization reversal for, e.g., computer technology, consists of the generation of a circularly polarized ac field of sufficient amplitude at the position of a nanoscale single-domain particle. In Ref. 25 a suggestion has been made to use the ac field generated by a superconducting weak link. If one is not turned off by the necessity to go

to lower temperatures (which is probably, inevitable for magnetic memory of ultra-high density), the advantage of this method would be the possibility to control the time dependence of the frequency by voltage across the link. Interaction between a nanomagnet and a Josephson junction has been subject of intensive research. Micro-SQUID setup has been used by Jamet et al to observe switching of the magnetization in a 3nm Co cluster^{26,27}, see also review 28. Ferromagnetic resonance in permalloy films grown on Nb substrate has been studied by Bell et al.²⁹ Petcović et al³⁰ investigated experimentally the direct dynamical coupling of spin modes and a supercurrent in a ferromagnetic junction, following theoretical study of this system by Houzet.³¹ Current-phase relation in a Josephson junction coupled with a magnetic dot has been investigated theoretically by Samokhvalov.³² Most of the research in this area focused on the proximity effect³³⁻³⁵ rather than on electromagnetic interaction.

In this paper we study magnetization dynamics of a single-domain uniaxial magnetic particle in zero static field, induced by a circularly polarized ac field of constant amplitude but variable frequency. The model is formulated in Section II. General properties of the magnetization reversal are studied in Section III. Numerical results for the time-linear frequency sweep are presented in Section IV where the phase diagrams are computed for the dependence of the magnetization switching on parameters. They are the frequency sweep rate, the amplitude of the ac field, the magnetic anisotropy field, and the damping parameter. Analytical results for the time-linear sweep, that are generally in good agreement with numerical results, are given in Section V A. In Section V B we obtain the exact analytical solution for non-linear time dependence of the frequency that provides the fastest magnetization reversal. The model in which circularly polarized ac field is generated by two superconducting weak links is studied in Section VI with account of the back effect of the dynamics of the magnetic moment on the links. Our conclusions and suggestions for experiment are presented in Section VII.

II. THE MODEL

The energy of a single-domain magnetic particle with an uniaxial anisotropy in a circularly-polarized ac field has the form

$$\mathcal{H} = -KV M_z^2 - VM_x h \cos \Phi(t) - VM_y h \sin \Phi(t). \quad (1)$$

Here K is the magnetic anisotropy constant, V is particle's volume, \mathbf{M} is the magnetization, h is the amplitude of the ac field, and $\Phi(t)$ is the phase related to the time-dependent frequency as

$$\dot{\Phi}(t) \equiv \omega(t). \quad (2)$$

One of the cases we consider is that of the frequency linearly changing with time,

$$\omega(t) = -vt, \quad (3)$$

where $\Phi(t) = -vt^2/2$. The other case that will be studied here is a non-linear time dependence of the frequency that provides the fastest magnetization reversal.

It is convenient to recast the problem in terms of a classical spin $\mathbf{s} = \mathbf{M}/M_s$, $|\mathbf{s}| = 1$, where M_s is the saturation magnetization. The Landau-Lifshitz equation of motion for this spin has the form

$$\dot{\mathbf{s}} = \gamma [\mathbf{s} \times \mathbf{H}_{\text{eff}}] - \alpha\gamma [\mathbf{s} \times [\mathbf{s} \times \mathbf{H}_{\text{eff}}]], \quad (4)$$

where γ is the gyromagnetic ratio, α is dimensionless damping coefficient and

$$\mathbf{H}_{\text{eff}} = -\frac{1}{V} \frac{\partial \mathcal{H}}{\partial \mathbf{M}} = 2ds_z \mathbf{e}_z + h\mathbf{e}_x \cos \Phi(t) + h\mathbf{e}_y \sin \Phi(t) \quad (5)$$

is the effective field. Here $d \equiv H_a = KM_s$ is the anisotropy field. In the initial state the spin points in the negative- z direction, $\mathbf{s}(-\infty) = -\mathbf{e}_z$.

Further it is convenient to switch to the coordinate frame rotating around the z axis together with the magnetic field, so that in this frame the magnetic field is static. As the result, in the new frame the spin acquires a rotation opposite to that of the ac field in the initial (laboratory) frame. Thus in the rotating frame the Landau-Lifshitz has the form

$$\dot{\mathbf{s}} = [\mathbf{s} \times (\gamma \mathbf{H}_{\text{eff}} + \boldsymbol{\Omega}(t))] - \alpha\gamma [\mathbf{s} \times [\mathbf{s} \times \mathbf{H}_{\text{eff}}]], \quad (6)$$

where

$$\mathbf{H}_{\text{eff}} = 2ds_z \mathbf{e}_z + h\mathbf{e}_x, \quad \boldsymbol{\Omega}(t) = \omega(t)\mathbf{e}_z. \quad (7)$$

III. GENERAL PROPERTIES OF THE MAGNETIZATION REVERSAL

With the sign choice in Eq. (3), the ac field at negative times is precessing in the same direction as the magnetic moment, thus it excites magnetic resonance and may cause magnetization reversal. In the ideal case, as we will see below, the resonance condition holds during the whole reversal. After the magnetic moment overcomes the barrier, $s_z > 0$, it changes its precession direction, and so does the ac field.

In the rotating frame, the field $\omega(t)/\gamma$ sweeping at a linear rate makes the problem resembling that of the Landau-Zener (LZ) effect that can be formulated in terms of the evolution of a classical spin described by a Larmor equation. There are three modifications, however: (i) uniaxial anisotropy and (ii) damping added to the model and (iii) sweeping $\omega(t)$ in the negative direction. Because of the latter, the initial state of the spin in the rotating frame is the high-energy state with s_z opposite to ω , see Eq. (3). To the contrast, in the regular LZ effect the initial spin state is the low-energy state. In the absence of anisotropy and damping, the initial orientation of the spin and the sweep direction do not matter. However, in the general case the situation does depend on these factors.

In particular, in the absence of damping one can multiply $\gamma \mathbf{h}_{\text{eff}} + \boldsymbol{\Omega}(t)$ by -1 that only makes the spin precess in the opposite direction but does not affect its reversal. The resulting model is a model with a positive sweep, such as the regular LZ problem, while the anisotropy becomes easy-plane, $d < 0$. It was shown³⁶ that in this case for a sweep slow enough the system adiabatically follows the time-dependent lowest-energy state and the spin switching is very efficient. In our original model (with $\alpha = 0$) the magnetization reversal is similar. Only instead of adiabatically following the lowest-energy state, the spin adiabatically follows the highest-energy state, in which it was at the beginning.

This adiabatic solution corresponds to the maximum of the energy in the rotating frame

$$\mathcal{H}/(VM_s) = -ds_z^2 - s_x h - (\omega/\gamma) s_z \quad (8)$$

The maximal energy corresponds to $s_y = 0$. Using $s_x = -\sqrt{1 - s_z^2}$ (opposite to the transverse field) and requiring $d\mathcal{H}/ds_z = 0$, one obtains the equation

$$2ds_z + hs_z/\sqrt{1 - s_z^2} + \omega/\gamma = 0 \quad (9)$$

for the energy maximum. Since in practical conditions $h \ll d$, an approximate solution of this 4th-order algebraic equation for the adiabatic spin value reads

$$s_z = \begin{cases} -1, & \omega > 2\gamma d \\ -\omega/(2\gamma d), & |\omega| \leq 2\gamma d \\ 1, & \omega < -2\gamma d. \end{cases} \quad (10)$$

Note that this solution is independent of h . Nonzero values of h cause rounding at the borders of the central region $|\omega| \leq 2\gamma d$ where the reversal occurs. In the laboratory frame, the spin is precessing during adiabatic reversal being phase-locked to the ac field.

For $\alpha = 0$ the magnetization reversal can be achieved for whatever small ac field h . In the case of a nonzero damping, there is a dissipative torque acting towards the energy minima, and the ac field h has to exceed a threshold value to overcome this torque. Below we will see that the magnetization reversal requires

$$h > \alpha d \quad (11)$$

that is much easier to fulfill than $h > 2d$ in the case of a static field. As the torque due to the transverse field is maximal when the magnetic moment is perpendicular to it, in the presence of damping the magnetic moment goes out of the x - z plane during the reversal.

IV. NUMERICAL - MAGNETIZATION REVERSAL BY THE TIME-LINEAR FREQUENCY SWEEP

A. Time dependences of reversing magnetization

The results of numerical solution of Eq. (6) in the undamped case $\alpha = 0$ for a small frequency sweep rate are

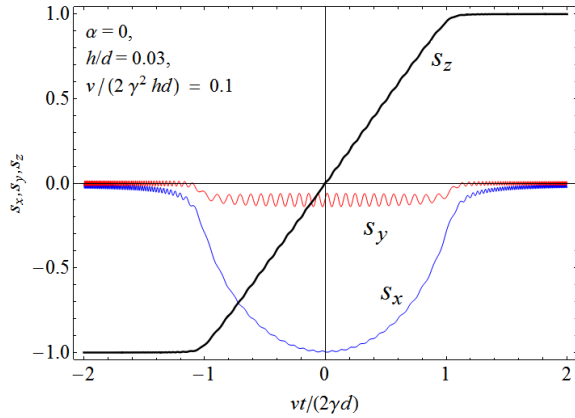


Figure 1: Almost adiabatic magnetization reversal at zero damping.

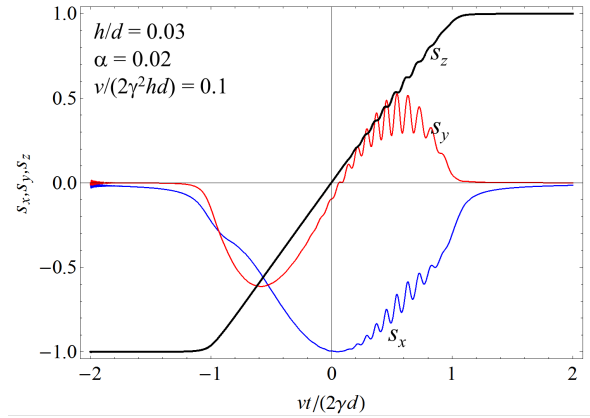


Figure 3: Almost adiabatic magnetization reversal for $\alpha = 0.02$.

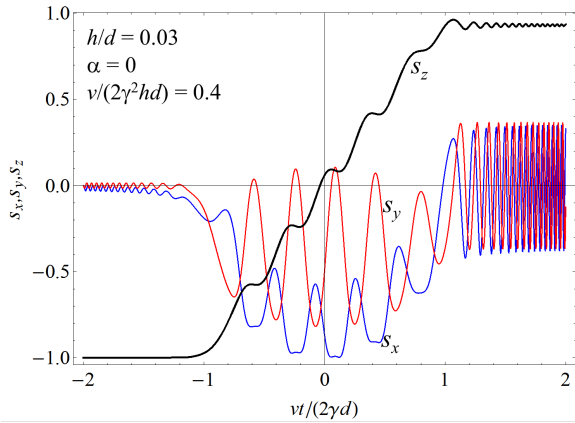


Figure 2: Non-adiabatic magnetization reversal at zero damping.

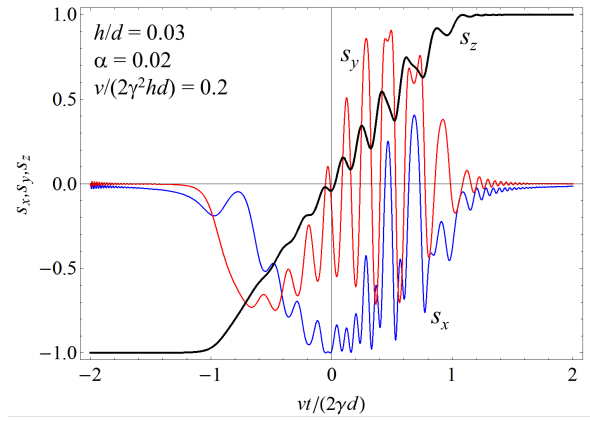


Figure 4: Non-adiabatic magnetization reversal for $\alpha = 0.02$.

shown in Fig. 1. Magnetization reversal in this case is almost adiabatic and $s_z(t)$ is well described by Eq. (10) with rounding at the borders of the reversal interval due to a small value of h/d . The reversal is practically confined to the z - x plane and s_y is small. Numerical results for a faster sweep rate are shown in Fig. 2. Here there is still magnetization reversal but it is not adiabatic and the final value of s_z is smaller than one. Because of this, the magnetic moment is precessing around the z axis, as manifested by s_x and s_y . During reversal the magnetization is substantially deviating from the z - x plane. For larger sweep rates the reversal quickly becomes impossible.

Fig. 3 shows that in the damped case the magnetic moment substantially deviates from the z - x plane. Still, overall the reversal in this case is close to adiabatic. Increasing the sweep rate leads to a non-adiabatic regime shown in Fig. 4. Here transverse spin components are oscillating and the dependence of s_z is jagged. This shows that, in the laboratory frame, the phase locking between the magnetic moment and the ac field is about to break.

In spite of all this, there is a complete reversal because the damping finally brings the magnetic moment to the bottom of the potential well (c.f. Fig. 2). For a faster sweep the reversal disappears and the magnetic moment lands in the initial well, $s_z = -1$. In the case of a slow sweep shown in Fig. 5 an instability can develop that leads to the breakdown of the phase locking and to faster relaxation of the magnetic moment towards one of the two potential wells. The final value of s_z (1 or -1) behaves irregularly vs sweep rate. This regime is not interesting for applications aimed at achieving as fast as possible reversal.

B. Phase diagram of the magnetization reversal by the time-linear frequency sweep

Dependence of the final value of s_z on the amplitude of the ac field h and frequency sweep rate v defines the “phase diagram” of the magnetization reversal. In the undamped case the numerically calculated phase diagram is shown in Fig. 6. The final s_z is color-coded: black corre-

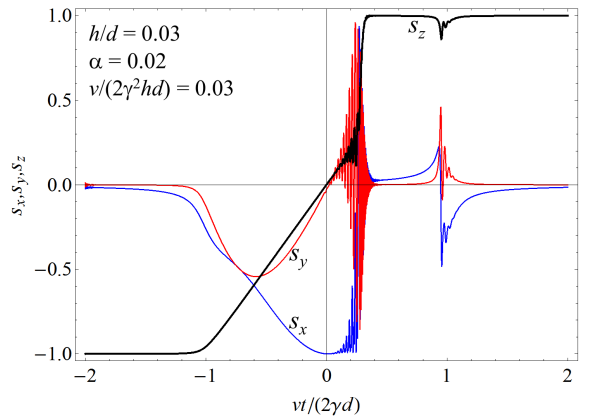


Figure 5: Instability in slow magnetization reversal for $\alpha = 0.02$.

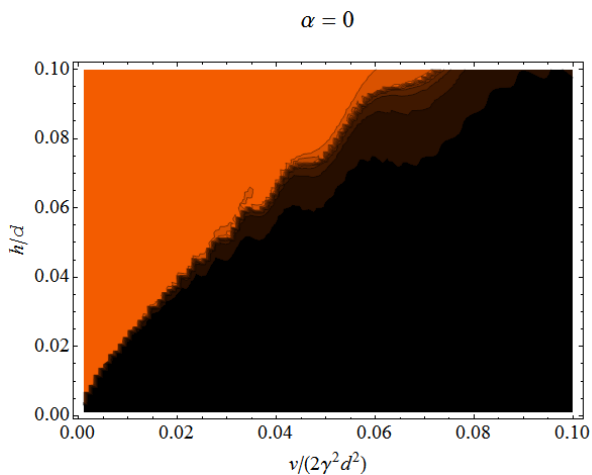


Figure 6: Phase diagram of the magnetization reversal in the undamped case.

sponds to $s_z = -1$ (non-reversal) and red corresponds to $s_z = 1$ (reversal). One can see that the reversal requires h sufficiently large and v sufficiently small. The curvature of the phase boundary at small h and v suggests a fractional power. Careful examination of this region of the phase diagram shows that the reversal condition has the form

$$\frac{v}{2\gamma^2 d^2} < c \left(\frac{h}{d}\right)^{4/3}, \quad c \simeq 1.6 \quad (12)$$

at $h/d \ll 1$ and $\alpha = 0$.

Phase diagram of the magnetization reversal in the damped case $\alpha = 0.02$ is shown in Fig. 7. It is similar to Fig. 6 but there is a threshold for the magnetization reversal on h and the phase-boundary line goes linearly at small v . Computations for different values of α suggest that the reversal requires $h/d > \alpha$.

One can compute other types of phase diagrams for the magnetization reversal that show a compact reversal region and the whole boundary line. The most

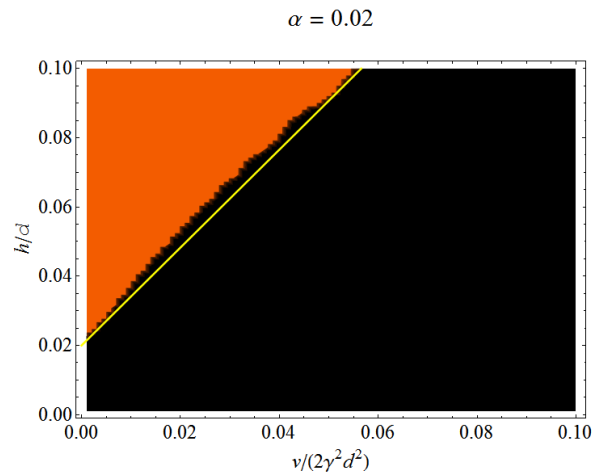


Figure 7: Phase diagram of the magnetization reversal for $\alpha = 0.02$. Yellow line: Eq. (26).

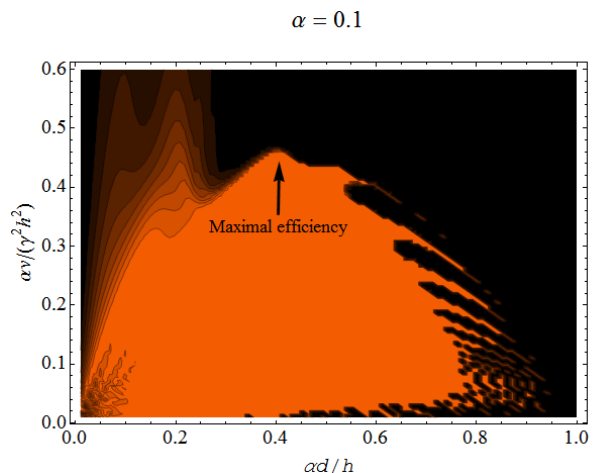


Figure 8: Efficiency-type phase diagram of the magnetization reversal for $\alpha = 0.1$.

useful of these phase diagrams uses the parameters $(\alpha d/h, \alpha v/(\gamma^2 h^2))$. Indeed, the area of the magnetization reversal is the compact region $0 < \alpha d/h < 1$ and v/h^2 is inversely proportional to the energy of the ac field injected during the time of the reversal by the linear frequency sweep

$$t_{\text{rev}}^{(\text{linear})} = \frac{2\gamma d}{v}. \quad (13)$$

The maximum of v/h^2 corresponds to the minimal injected energy and thus to the maximal efficiency of the reversal. Figs. 8 and 9 show that the maximal efficiency of the time-linear frequency sweep corresponds to $\alpha d/h \approx 0.5$. Also in these figures one can see that there is no reversal if the sweep rate is too low, especially for low ac fields on the right side.

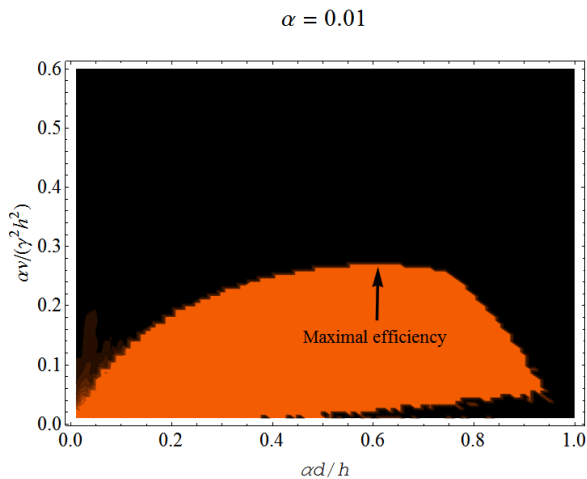


Figure 9: Efficiency-type phase diagram of the magnetization reversal for $\alpha = 0.01$.

V. ANALYTICAL

Analytical investigation of the magnetization reversal is more convenient in spherical coordinates

$$s_z = \cos \theta, \quad s_x = \sin \theta \cos \varphi, \quad s_y = \sin \theta \sin \varphi. \quad (14)$$

After neglecting the ac field in the dissipation term, Eq. (6) becomes

$$\dot{\theta} = \gamma h \sin \varphi - \alpha \gamma d \sin 2\theta \quad (15)$$

$$\dot{\varphi} = -2\gamma d \cos \theta - \omega(t) + \gamma h \cos \varphi \cot \theta. \quad (16)$$

A. Linear frequency sweep

In the case of a linear frequency sweep, Eq. (3), one can rewrite the equation of motion for the spin in terms of the dimensionless time variable

$$\tau = vt/(2\gamma d). \quad (17)$$

The resulting equation of motion has the form

$$d\theta/d\tau = b \sin \varphi - \alpha a \sin 2\theta \quad (18)$$

$$d\varphi/d\tau = -2a(\cos \theta - \tau) + b \cos \varphi \cot \theta, \quad (19)$$

where

$$a \equiv \frac{2\gamma^2 d^2}{v}, \quad b \equiv \frac{2\gamma^2 dh}{v} \quad (20)$$

characterise the sweep rate. Another important parameter is

$$A = \alpha d/h. \quad (21)$$

Since a is a large parameter, phase locking of the magnetic moment to the ac field and thus efficient reversal

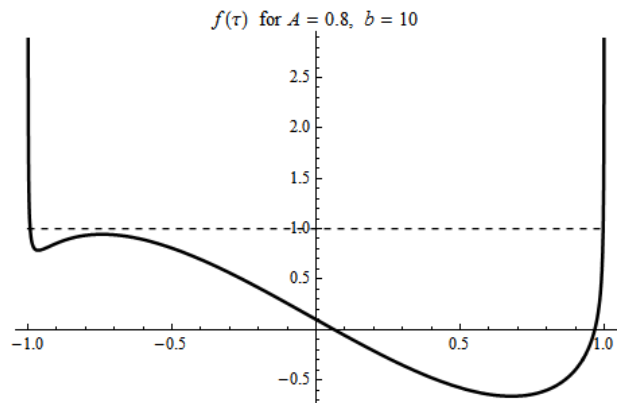


Figure 10: $f(\tau)$ of Eq. (24).

requires $\cos \theta \cong \tau$ in the reversal region $|\tau| < 1$. If $\cos \theta$ only slightly deviates from this form, this causes strong oscillations of φ and thus the breakdown of the phase locking. Setting $\cos \theta = \tau$, from Eq. (18) one obtains the phase-locking condition for φ in the form

$$\sin \varphi = \frac{1}{b} \frac{d\theta}{d\tau} + A \sin 2\theta. \quad (22)$$

The term on the left of this formula is proportional to the torque acting on the spin from the ac field. This torque has to ensure temporal change of θ (i.e., reversal) and compensate for the dissipative torque that is acting toward potential wells. One can see that damping hampers climbing the barrier by the magnetic moment. The maximal damping torque is realized at $\theta = 3\pi/4$, where $\sin 2\theta = -1$. Since the reversal implies $d\theta/d\tau < 0$, it is clear that for $A > 1$ the ac torque cannot overcome the damping torque. Thus, the necessary condition for the magnetization reversal is

$$A < 1, \quad (23)$$

while the more restricting sufficient condition requires that the right-hand side of Eq. (22) does not drop below -1 for all τ . The latter requires the frequency sweep rate to be not too fast. Using $\cos \theta = \tau$, one can rewrite this condition in the form

$$\max f(\tau) < 1, \quad f(\tau) \equiv -2A\tau\sqrt{1-\tau^2} + \frac{1}{b\sqrt{1-\tau^2}}. \quad (24)$$

Because of the inertial term, $f(\tau)$ shown in Fig. 10 diverges at the borders of the reversal interval. This is, however, an artefact of neglecting the rounding of the dependence $s_z(\tau)$ at $\tau = \pm 1$ because of the finite value of h . When this effect is taken into account, there are maxima around $\tau = \pm 1$ instead of divergences. Thus, spin reversal can break down either because of the inertial effect near $\tau = -1$ or because of the effect of dissipation near $\theta = 3\pi/4$, i.e., $\tau = -1/\sqrt{2}$, depending on which one occurs at a smaller sweep rate.

Let us first consider the dissipative breakdown of the magnetization reversal for A slightly below 1 that happens at a small sweep rate. In this case $1/b \propto v$ is small and the second term in $f(\tau)$ in Eq. (24) is a perturbation. Thus the value of this term can be taken at the unperturbed dissipative maximum $\tau = -1/\sqrt{2}$. Using $-2\tau\sqrt{1-\tau^2} = 1$ and $\sqrt{1-\tau^2} = 1/\sqrt{2}$, one obtains the reversal condition

$$A + \frac{\sqrt{2}}{b} < 1. \quad (25)$$

This can be rewritten in real units as

$$\frac{v}{2\gamma^2 d^2} < \frac{1}{\sqrt{2}} \left(\frac{h}{d} - \alpha \right) \quad (26)$$

and it is in a reasonable agreement with the numerical results in Fig. 7. Although this expression formally survives in the dissipationless limit $\alpha \rightarrow 0$, it becomes inapplicable in this limit. Here the breakdown of spin reversal is due to the inertial effect.

To investigate the latter, one needs a more accurate approximation for $f(\tau)$ in Eq. (24) near $\tau = -1$ that transforms divergence into a maximum. This can be done by solving Eq. (9) although it is difficult to do it analytically in general. Instead, since the maximum should be close to $\tau = -1$, we can solve this equation exactly at $\tau = -1$, which is much easier. A perturbative solution for $h/d \ll 1$ yields

$$d\dot{s}/d\tau \cong 2/3, \quad \sin\theta \cong (h/d)^{1/3}. \quad (27)$$

and then one obtains

$$-\frac{d\theta}{d\tau} = \frac{1}{\sin\theta} \frac{d\cos\theta}{d\tau} = \frac{2}{3} \left(\frac{d}{h} \right)^{1/3}. \quad (28)$$

Replacing in Eq. (24) $1/\sqrt{1-\tau^2}$ by this result and using Eq. (20), one obtains the dissipationless reversal condition

$$\frac{v}{2\gamma^2 d^2} < \frac{3}{2} \left(\frac{h}{d} \right)^{4/3}, \quad (29)$$

in a reasonable agreement with the numerical result, Eq. (12).

The combined reversal condition obtained from Eqs. (26) and (12) is thus

$$\frac{v}{2\gamma^2 d^2} < \min \left\{ \frac{1}{\sqrt{2}} \left(\frac{h}{d} - \alpha \right), \frac{3}{2} \left(\frac{h}{d} \right)^{4/3} \right\}. \quad (30)$$

Let us shortly discuss the stability of our spin-reversal solutions that, in the laboratory frame, is the stability of phase locking between the spin and the ac field at slow frequency sweep. Linearizing Eqs. (15) and (16) around the static solution (θ, φ) at a fixed time, one obtains the deviation $(\delta\theta, \delta\varphi) \propto e^{\lambda t}$. For the orientations closer to the wells, $3\pi/4 < \theta \leq \pi$ and $0 \leq \theta < \pi/4$, one has $\lambda < 0$

and phase locking is stable. However, for the orientations closer to the barrier, $\pi/4 < \theta < 3\pi/4$, one has $\lambda > 0$ and phase locking is unstable. Thus the barrier has to be crossed fast enough during reversal before the instability develops. Considering the process quasi-statically, one can write

$$(\delta\theta, \delta\varphi) \sim \exp \left[\int_{t_0}^t dt' \lambda(t') \right] \quad (31)$$

and use the stability criterion $\int_{t_0}^0 dt \lambda(t) < 1$, where t_0 is the time of entering the instability region and the top of the barrier is reached at $t = 0$. After some algebra one arrives at the stability criterium

$$\frac{\alpha}{3\sqrt{2}} < \frac{v}{2\gamma^2 d^2}. \quad (32)$$

A boundary of this kind is seen in Figs. 8 and 9 close to the bottom.

B. Optimal frequency sweep

The magnetization reversal can be optimized by applying a time-nonlinear frequency sweep. Among all possible cases the so-called ‘‘optimal sweep’’ stands out as a rotation of the magnetic moment in one plane (in the rotating frame) with $\varphi = -\pi/2$, that is with the moment being always perpendicular to the ac field. It is easy to see that this provides the maximal torque on the magnetization during the reversal. With

$$\omega(t) = -2\gamma d \cos\theta \quad (33)$$

Eq. (16) self-consistently yields $\dot{\varphi} = 0$. Then Eq. (15) takes the form

$$\dot{\theta} = -\gamma h - \alpha \gamma d \sin 2\theta. \quad (34)$$

Integrating this equation with the initial condition $\theta(0) = \pi$, one obtains

$$\tan\theta = \frac{-\sin(\tilde{t})}{\cos(\tilde{t} - \arcsin A)}, \quad (35)$$

where $\tilde{t} \equiv \sqrt{1 - A^2} \gamma h t$ and A is defined by Eq. (21). After some algebra the expression for the optimal sweep can be transformed to the most convenient form:

$$s_z = \cos\theta = -\frac{\cos(\tilde{t} - \arcsin A)}{\sqrt{1 - A \cos(2\tilde{t} + \arccos A)}} \quad (36)$$

illustrated in Fig. 11. Together with Eq. (33) it gives a non-linear time dependence of the frequency of the ac field that provides the fastest reversal of the magnetic moment. This exact result, that generalizes the result of

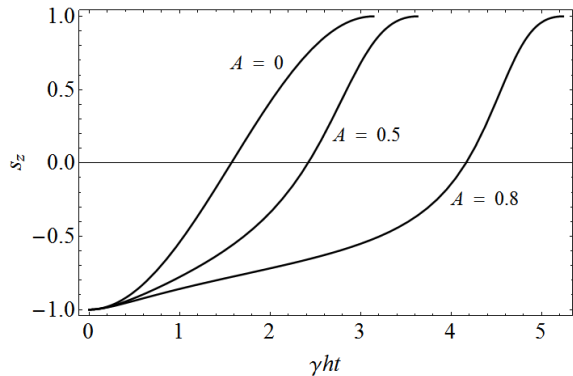


Figure 11: Optimal magnetization reversal for different values of $A = \alpha d/h$.

Ref. 24 obtained in the absence of damping, must have important practical applications.

In the dissipationless case, $A \rightarrow 0$, the optimal magnetization reversal is described by a pure cosine function that is a Rabi precession of the magnetic moment around the ac field. In the general case, the reversal is mainly due to the cos term in the numerator, whereas the denominator only affects the shape of the switching curve, making it non-sinusoidal in the presence of damping.

Eq. (36) and Fig. 11 describe the optimal reversal during the time

$$t_{\text{rev}} = \frac{\pi}{\sqrt{1 - A^2}\gamma h}, \quad A \equiv \frac{\alpha d}{h} < 1 \quad (37)$$

It is instructive to compare this time with the time of the magnetization reversal for the linear sweep, defined by Eq. (13) (notice that the total time of the process may be longer). In the dissipationless case, the maximal sweep speed is given by Eq. (12). For that speed one obtains the minimal reversal time

$$t_{\text{rev}}^{(\text{linear})} = \frac{4}{3\gamma h} \left(\frac{d}{h}\right)^{1/3} \quad (38)$$

that is longer than the time given by Eq. (37) with $A = 0$. In the dissipative case near $A = 1$, the maximal sweep rate for the linear sweep follows from Eq. (26). This yields

$$t_{\text{rev}}^{(\text{linear})} = \frac{2\sqrt{2}}{\gamma h} \frac{1}{1 - A}. \quad (39)$$

For $|1 - A| \ll 1$ this is also much longer than the time given by Eq. (37). In the relevant region $A \sim 1$ Eqs. (37) and (39) are comparable. However, one has to keep in mind that the linear frequency sweep has to begin with a frequency beyond the resonance range, so that the actual reversal time of the linear sweep is somewhat longer than above.

The total energy input of the ac power needed for the reversal satisfies

$$E \propto h^2 t_{\text{rev}}. \quad (40)$$

For the optimal sweep one has

$$E \propto \frac{h}{\sqrt{1 - A^2}} = \frac{h^2}{\sqrt{h^2 - (\alpha d)^2}}. \quad (41)$$

The minimum of this function, $2\alpha d$, is achieved at

$$h = \sqrt{2}\alpha d \quad (42)$$

(that is at $A = \alpha d/h = 1/\sqrt{2}$).

For the linear sweep one has

$$E^{(\text{linear})} \propto h^2 t_{\text{rev}}^{(\text{linear})} = \frac{h}{1 - A} = \frac{h^2}{h - \alpha d}. \quad (43)$$

The minimum of this function, $4\alpha d$, is achieved at

$$h = 2\alpha d \quad (44)$$

(that is, at $A = \alpha d/h = 0.5$).

We see that the magnetization reversal by the optimal sweep requires both a smaller amplitude of the ac field and a smaller total energy input, as compared to the linear sweep. In both cases the injected energy at the maximal efficiency is proportional to α and thus the efficiency itself is inversely proportional to α . (The latter was multiplied by α in Figs. 8 and 9 to make them approximately scale with α .)

VI. REVERSAL OF THE MAGNETIZATION BY JOSEPHSON CURRENTS

Pointed switching of the magnetization of a nanomagnet by the ac field of varying frequency may be achieved by coupling the magnet to a weak superconducting link²⁵. Advantage of this method consists of the possibility to control the time dependence of the frequency by the voltage across the link, $V(t)$. As has been discussed in the Introduction the most effective switching occurs when the ac field is circularly polarized. This requires two weak links shown in Fig. 12. In addition to the previous problem one should now take into account the back effect of the magnet on the weak links. As we shall see below, our results for the optimal sweep permit generalization that provides exact time dependences of voltages on the two links needed to obtain full reversal of the magnetization.

Each superconducting weak link interacting with the magnet contributes the term

$$\mathcal{E}_J = -E_J \cos \left[\delta - \frac{2\pi}{\Phi_0} \int_1^2 d\mathbf{r} \cdot \mathbf{A}(\mathbf{r}, t) \right] \quad (45)$$

to the total energy. Here $E_J = \hbar I_c / (2e)$ is the Josephson energy of the link, with I_c being the critical current. The argument of cosine is the gauge invariant phase that consists of two contributions. The first contribution satisfying $\dot{\delta} = 2eV(t)/\hbar$ comes from the voltage across the link, while the second contribution is due to the vector

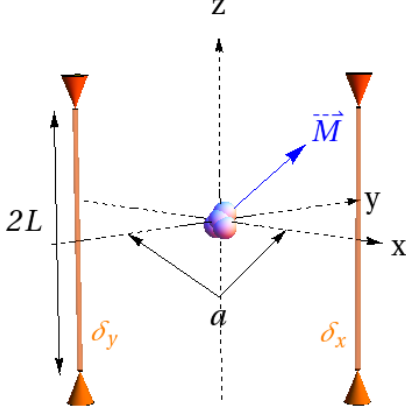


Figure 12: Geometry used in the model: Nanomagnet makes the right angle with two parallel superconducting weak links of length $2L$ at a distance a from the magnet.

potential of the magnet integrated between the terminals of the link; $\Phi_0 = 2\pi\hbar c/(2e)$ being the flux quantum. Following the footsteps of Ref. 25, it is easy to show that interaction of the magnet with two Josephson junctions leads to a modified expression (5) for the effective field,

$$\mathbf{H}_{\text{eff}} = 2ds_z\mathbf{e}_z + h_J[\sin(\delta_y - ks_x)\mathbf{e}_x + \sin(\delta_x - ks_y)\mathbf{e}_y] \quad (46)$$

where $h_J = kE_J/(M_sV)$ is the amplitude of the ac magnetic field created by the junction at the position of the nanomagnet,

$$\frac{d\delta_{x,y}}{dt} = \frac{2eV_{x,y}}{\hbar}, \quad (47)$$

$V_{x,y}$ are the voltages across the junctions, and

$$k = \frac{4\pi M_s V}{\alpha\Phi_0} \frac{L}{\sqrt{L^2 + a^2}} \quad (48)$$

is a dimensionless spin-feedback coupling coefficient.

For the time-linear voltage, dependence of the effective field in Eq. (46) on oscillating transverse spin components is detrimental for reversal. This happens because the oscillating additions to the otherwise time-smooth phases disturb phase locking between the magnetization and the ac field and cause non-adiabaticity. Fig. 13 shows that non-adiabaticity in the zero-damping case becomes pronounced already for small values of the feedback coefficient k . In the realistic damped case the negative influence of finite k is even stronger. The instability of the phase locking for $\pi/4 < \theta < 3\pi/4$ discussed at the end of Sec. V A exponentially increases the mismatch between the directions of the ac field and the magnetization arising because of the feedback. As a result, the magnetization randomly lands in one of the two wells, as shown in Fig. 14.

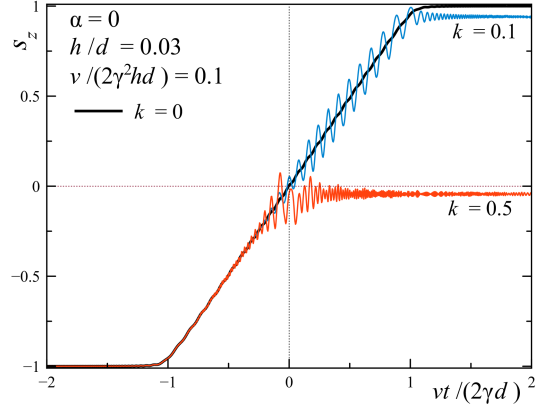


Figure 13: Detrimental influence of the magnetization feedback on the Josephson junction in the case of linear frequency sweep and zero damping.

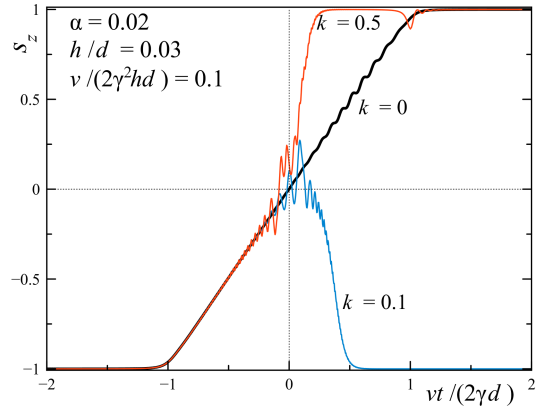


Figure 14: Influence of the magnetization feedback in the damped case with linear sweep.

In order to reduce the effect of the Josephson junctions on the magnet to the effect of a circularly polarized field, one can require that

$$\delta_x - ks_y = \delta(t), \quad \delta_y - ks_x = \delta(t) + \frac{\pi}{2}, \quad (49)$$

where $\delta(t)$ is a phase. This allows one to use the results of the previous section for the optimal sweep requiring $\dot{\delta}(t) = \omega(t) = -2\gamma d \cos \theta$. For such a sweep, $s_{x,y}(t)$ in the laboratory frame are precessing during reversal as follows

$$s_x = \sin \theta(\tilde{t}) \cos \delta(\tilde{t}) = \frac{\sin(\tilde{t}) \cos \delta(\tilde{t})}{\sqrt{1 - A \cos(2\tilde{t} + \arccos A)}} \\ s_y = \sin \theta(\tilde{t}) \sin \delta(\tilde{t}) = \frac{\sin(\tilde{t}) \sin \delta(\tilde{t})}{\sqrt{1 - A \cos(2\tilde{t} + \arccos A)}}, \quad (50)$$

where $A = \alpha d/h_J$, $\tilde{t} = \sqrt{1 - A^2}\gamma h_J t$, and $\sin \theta(\tilde{t})$ was

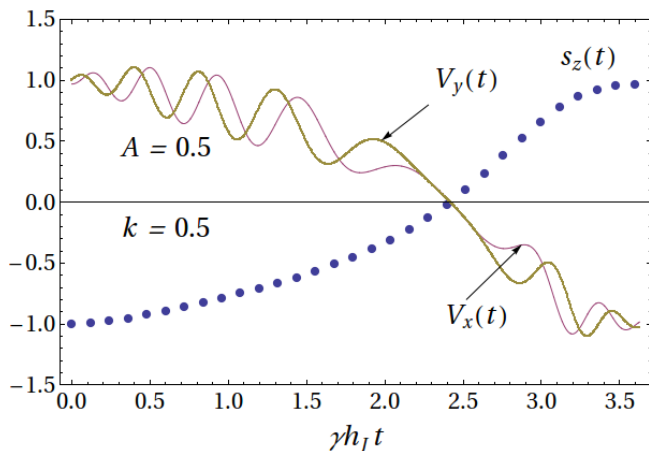


Figure 15: The optimal choice of V_x (purple) and V_y (gold) across the weak links at $A = k = 0.5$. Time dependence of s_z is shown by blue dots.

obtained by combining Eqs. (35) and (36). The time-dependent phase is given by

$$\delta(t) = \int_0^t \omega(t') dt' = -\frac{2d/h_J}{\sqrt{1-A^2}} \int_0^t \cos \theta(\tilde{t}') d\tilde{t}'. \quad (51)$$

with $\omega(t)$ defined by Eqs. (33) and $\theta(t)$ given by (36). In accordance with Eq. (49), the optimal time dependence of the voltages across the junctions become

$$V_x(t) = \frac{\hbar}{2e} [\omega(t) + k\dot{s}_y], \quad V_y(t) = \frac{\hbar}{2e} [\omega(t) + k\dot{s}_x]. \quad (52)$$

This dependence is shown in Fig. 15. The time dependence of s_z in the figure is the same as for the optimal frequency sweep in Fig. 11. Oscillations of the voltages are due to the terms in Eq. (52) that depend on $s_{x,y}$. They are weak as long as k is small. Oscillations disappear in the limit of $k \rightarrow 0$, making $V_{x,y}$ in that limit to follow the smooth time dependence of the optimal frequency sweep obtained in the previous section.

Having practical applications in mind, it is interesting to test the stability of the reversal described by the above equations against high-frequency voltage noise. This can be done by writing

$$V'_{x,y}(t) = V_{x,y}(t) + \epsilon \frac{\hbar \gamma d}{e} F_{x,y}(t) \quad (53)$$

with $F_{x,y}$ being uniform random functions of time between -1 and $+1$ and ϵ representing the relative strength of the noise. Quite remarkably, as is illustrated in Fig. 16, the full magnetization reversal may occur even in the presence of a strong noise. At $\epsilon = 1$ this happens with more than 0.99 probability. With less than 0.01 probability the magnetic moment bounces back to $s_z = -1$ before it reaches $s_z = 1$. This can be traced to the fact that the high-frequency noise in most cases averages out in the phase δ because the latter is proportional to the time integral of the voltage.

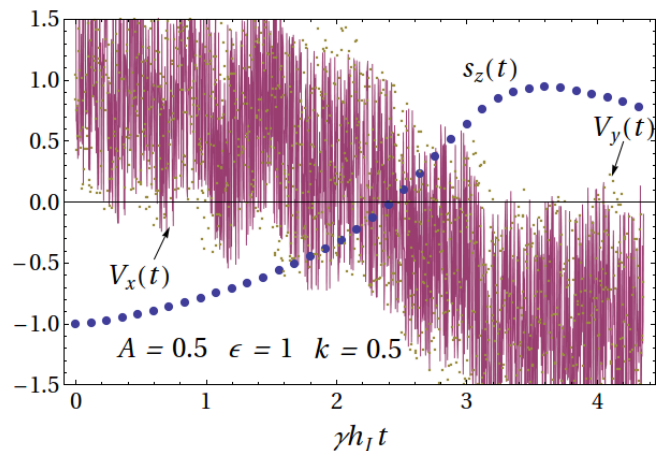


Figure 16: Optimal magnetization reversal in the presence of voltage noise in the weak links.

VII. DISCUSSION AND CONCLUSIONS

We have studied numerically and analytically a microwave-assisted reversal of the magnetic moment of a single-domain magnetic particle. We conclude from our studies that a circularly polarized ac field that has specific time dependence of the frequency can be an effective tool for switching the magnetization. The corresponding physical mechanism consists of the resonant absorption of photons of the spin projection that ensures the consistent change in the projection of the magnetic moment. Emission of excitations by the magnetic moment inhibits this process. In the micromagnetic theory it is described by the phenomenological dimensionless small parameter α that can be independently measured. In single-domain particles this parameter is usually greater than in bulk materials and is typically of order $0.01 - 0.1$.³⁷ The condition on the power of the ac field needed to overcome damping and reverse the magnetization is $h > \alpha d$. For, e.g., the anisotropy field d of order 0.01 T and α of order 0.01 , one obtains h of order 0.0001 T for the amplitude of the ac field, which is a reasonable value from the practical point of view.

We have studied linear and nonlinear time dependence of the frequency of the ac field. It has been demonstrated that the linear case, $\omega = -vt$, resembles the Landau-Zener problem. Magnetization reversal has been demonstrated numerically and the phase diagrams have been obtained that show the range of v , h , d , and α that provide the reversal. They show that for the reversal to occur, the frequency sweep must be sufficiently slow, but not too slow when the damping is finite. The linear case has also been studied analytically. Condition (30) has been obtained for the upper bound on the frequency sweep rate. For the values of the parameters used above, that upper bound is in the ballpark of 10^7 GHz/s. The minimal reversal time for the time-linear sweep is of order $(\gamma h)^{-1}$.

We have also studied a time-nonlinear frequency sweep. Exact analytical solution for $\omega(t)$ that provides the fastest reversal has been obtained with account of damping. It is given by equations (33) and (36). This finding may have important practical application. We call this sweep the optimal sweep. It has been demonstrated that, besides ensuring the fasted magnetization switch, it also pumps less energy into the system as compared to the linear sweep. In both cases the injected energy is proportional to α .

Circularly polarized ac field can be generated by coupling a single-domain particle electromagnetically to two weak superconducting links whose phases are displaced by $\pi/2$ with respect to each other. One advantage of such a system is that the time dependence of the frequency of the ac field generated by the links can be controlled by voltage. This problem has been studied by us with ac-

count of the back effect of the magnetic moment on the links. Magnetization reversal has been demonstrated numerically and analytical expressions have been derived for the time dependence of the voltages across the links that provide the fasted magnetization reversal. One remarkable property of this system is weak dependence of the reversal dynamics on the voltage noise.

VIII. ACKNOWLEDGEMENTS

D.G. is thankful to H. Kachkachi, N. Barros, and C. Thirion for useful discussions of microwave-induced spin reversal.

This work has been supported by the U.S. Department of Energy through Grant No. DE-FG02-93ER45487.

-
- ¹ C. H. Back, D. Weller, J. Heidmann, D. Mauri, D. Guarisco, E. L. Garwin, and H. C. Siegmann, *Phys. Rev. Lett.* **81**, 3251 (1998).
 - ² H. W. Schumacher, C. Chappert, P. Crozat, R. C. Sousa, P. P. Freitas, J. Miltat, J. Fassbender, and B. Hillebrands, *Phys. Rev. Lett.* **90**, 017201 (2003).
 - ³ C. Thirion, W. Wernsdorfer, and D. Maily, *Nature Materials* **2**, 524 (2003).
 - ⁴ E. M. Chudnovsky and J. Tejada, *Lectures on Magnetism* (Rinton Press, Princeton, NJ, 2008).
 - ⁵ Z. Z. Sun and X. R. Wang, *Phys. Rev. B* **74**, 132401 (2006).
 - ⁶ J. Grollier, M. V. Costache, C. H. van der wal, and B. J. van Wees, *J. Appl. Phys.* **100**, 024316 (2006).
 - ⁷ H. T. Nembach, P. M. Pimentel, S. J. Hermsdoerfer1, B. Leven, B. Hillebrands, and S. O. Demokritov, *Appl. Phys. Lett.* **90**, 062503 (2007).
 - ⁸ Y. Nozaki, M. Ohta, S. Taharazako, K. Tateishi, S. Yoshimura, and K. Matsuyama, *Appl. Phys. Lett.* **91**, 082510 (2007).
 - ⁹ T. Moriyama, R. Cao, J. Q. Xiao, J. Lu, X. R. Wang, Q. Wen, and H. W. Zhang, *Appl. Phys. Lett.* **90**, 152503 (2007).
 - ¹⁰ J. Podbielski, D. Heitmann, and D. Grundler, *Phys. Rev. Lett.* **99**, 207202 (2007).
 - ¹¹ G. Woltersdorf and C. H. Back, *Phys. Rev. Lett.* **99**, 227207 (2007).
 - ¹² Y. Wang, Y. Tang, and J-G. Zhu, *J. Appl. Phys.* **105**, 07B902 (2009).
 - ¹³ H. T. Nembach, H. Bauer, J. M. Shaw, M. L. Schneider, and T. J. Silva, *Appl. Phys. Lett.* **95**, 062 (2009).
 - ¹⁴ Z. Wang, K. Sun, W. Tong, M. Wu, M. Liu, and N. X. Sun, *Phys. Rev. B* **81** 064402 (2010).
 - ¹⁵ G. Bertotti, I. D. Mayergoyz, C. Serpico, M. d'Aquino, and R. Bonin, *J. Appl. Phys.* **105**, 07B712 (2009).
 - ¹⁶ G. Bertotti, C. Serpico, and I. D. Mayergoyz, *Phys. Rev. Lett.* **86**, 724 (2001).
 - ¹⁷ G. Bertotti, I. D. Mayergoyz, and C. Serpico, *J. Appl. Phys.* **91**, 7556 (2002).
 - ¹⁸ S. I. Denisov, T. V. Lyutyy, and P. Hänggi, *Phys. Rev. Lett.* **97**, 227202 (2006).
 - ¹⁹ M. Igarashi, Y. Suzuki, H. Miyamoto, Y. Maruyama, and Y. Shiroishi, *J. Appl. Phys.* **105**, 07B907 (2009).
 - ²⁰ S. Okamoto, M. Igarashi, N. Kikuchi, and O. Kitakami, *J. Appl. Phys.* **107**, 123914 (2010).
 - ²¹ N. Barros, M. Rassam, H. Jirari, and H. Kachkachi, *Phys. Rev. B* **83**, 144418 (2011).
 - ²² V. I. Yukalov and E. P. Yukalova, *J. Appl. Phys.* **111**, 023911 (2012).
 - ²³ I. Mayergoyz, M. Dimian, G. Bertotti, and C. Serpico, *J. Appl. Phys.* **95**, 7004 (2004).
 - ²⁴ K. Rivkin and J. B. Ketterson, *Appl. Phys. Lett.* **89**, 252507 (2006).
 - ²⁵ L. Cai and E. M. Chudnovsky, *Phys. Rev. B* **82**, 104429 (2010).
 - ²⁶ M. Jamet, W. Wernsdorfer, C. Thirion, D. Maily, V. Dupuis, P. Mélinon, and A. Pérez, *Phys. Rev. Lett.* **86**, 4676 (2001).
 - ²⁷ W. Wernsdorfer, *Adv. Chem. Phys.* **118**, 99 (2001).
 - ²⁸ W. Wernsdorfer, *Superconductor Science & Technology* **22**, 064013 (2009).
 - ²⁹ C. Bell, S. Milikisyants, M. Huber, and J. Aarts, *Phys. Rev. Lett.* **100**, 047002 (2008).
 - ³⁰ I. Petković, M. Aprili, S. E. Barnes, F. Beuneu, and S. Maekawa, *Phys. Rev. B* **80**, 220502(R) (2009).
 - ³¹ M. Houzet, *Phys. Rev. Lett.* **101**, 057009 (2008).
 - ³² A. V. Samokhvalov, *Phys. Rev. B* **80**, 134513 (2009).
 - ³³ See, e.g., review: A. I. Buzdin, *Rev. Mod. Phys.* **77**, 935 (2005).
 - ³⁴ A. Buzdin, *Phys. Rev. Lett.* **101**, 107005 (2008).
 - ³⁵ F. Konschelle and A. Buzdin, *Phys. Rev. Lett.* **102**, 017001 (2009).
 - ³⁶ D. A. Garanin, *Phys. Rev. B* **68**, 014414 (2003).
 - ³⁷ W. T. Coffey, D. S. F. Crothers, J. L. Dormann, Yu. P. Kalmykov, E. C. Kennedy, and W. Wernsdorfer, *Phys. Rev. B* **80**, 5655 (1998).